Supporting information

$Na_3LaP_2O_8$-enabled microstructural engineering for enhanced mechanical robustness and ionic transport behavior in NaSICON solid electrolytes

Xingyu Liu[1], Jürgen Peter Gross[1], Qianli Ma[2], Frank Tietz[2, 3], Jürgen Malzbender[1], Ruth Schwaiger[1]

[1]*Forschungszentrum Jülich GmbH, Institute of Energy Materials and Devices, Structure and Function of Materials (IMD-1), 52425 Jülich, Germany*

[2]*Forschungszentrum Jülich GmbH, Institute of Energy Materials and Devices, Materials Synthesis and Processing (IMD-2), 52425 Jülich, Germany*

[3]*Forschungszentrum Jülich GmbH, Institute of Energy Materials and Devices, Helmholtz Institute Münster-Ionics in Energy Storage (IMD-4), 52425 Jülich, Germany*

[*]Corresponding author: Xingyu Liu, e-mail: xing.liu@fz-juelich.de

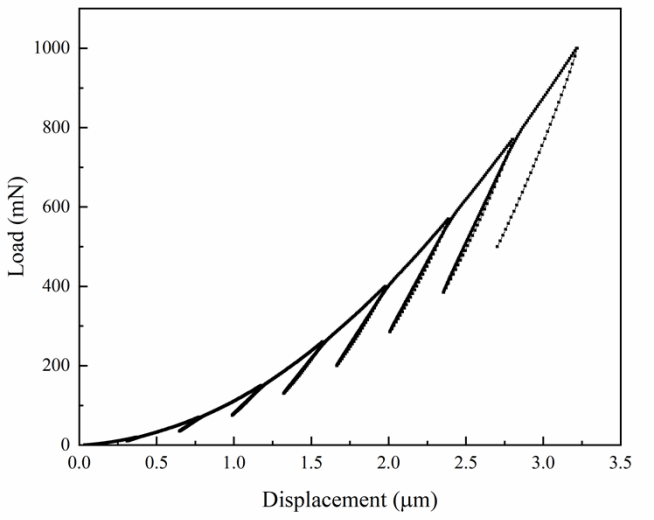

Fig. S1. Typical cyclic load-displacement curve.

The curve in Fig. S1 demonstrates the progressive loading–unloading behavior used to determine the elastic modulus (*E*) and hardness (*H*) of the samples. The use of multiple loading–unloading cycles provides several unloading segments, improving the stability and repeatability of the contact stiffness. The gradual increase in maximum load also minimizes the influence of surface roughness and surface-layer effects, allowing the extracted mechanical properties to better reflect the intrinsic behavior of the material.

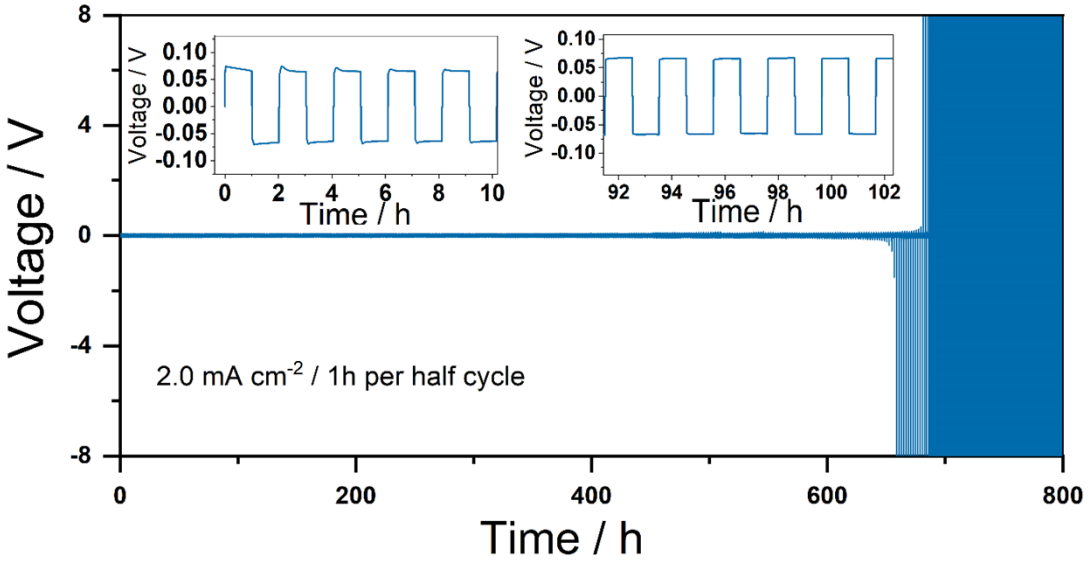

Fig. S2. Galvanostatic cycling of a Na | NZSP-2.5NLP | Na symmetric cell at 2.0 mA cm^{-2}, 2 mAh cm^{-2} (per half cycle) at RT. Data derived from *J. Power Sources* 626 (2025) 235773. [1] NZSP-2.5NLP exhibits reliable long-term stability.

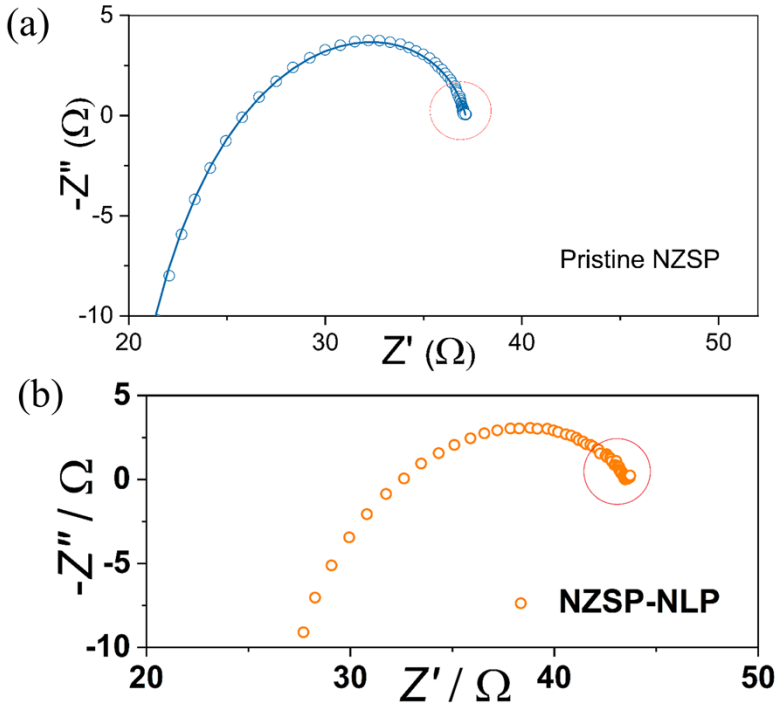

Fig. S3. Impedance spectra of symmetric cells. (a) Na | original NZSP | Na, derived from *Adv. Energy Mater.* 202201680, [2] and (b) Na | NZSP-2.5NLP | Na, derived from *J. Power Sources* 626 (2025) 235773. [1]

Fig. S3 shows the impedance spectra of Na | original NZSP | Na and Na | NZSP-2.5NLP | Na symmetric cells. Both of them show very good interfacial compatibility with sodium metal. The interfacial resistances are both "0" because they are almost not readable under impedance spectra (see the low frequency area in the red circle).

However, since it is known that Na dendrite formation is mainly started from the position of grain-boundaries, as shown in the figure below (Fig. S4, derived from *Adv. Energy Mater.* 202201680). The reinforced microstructure of the grain-boundary of NZSP-NLP is surely beneficial for the prevention of dendrite formation.

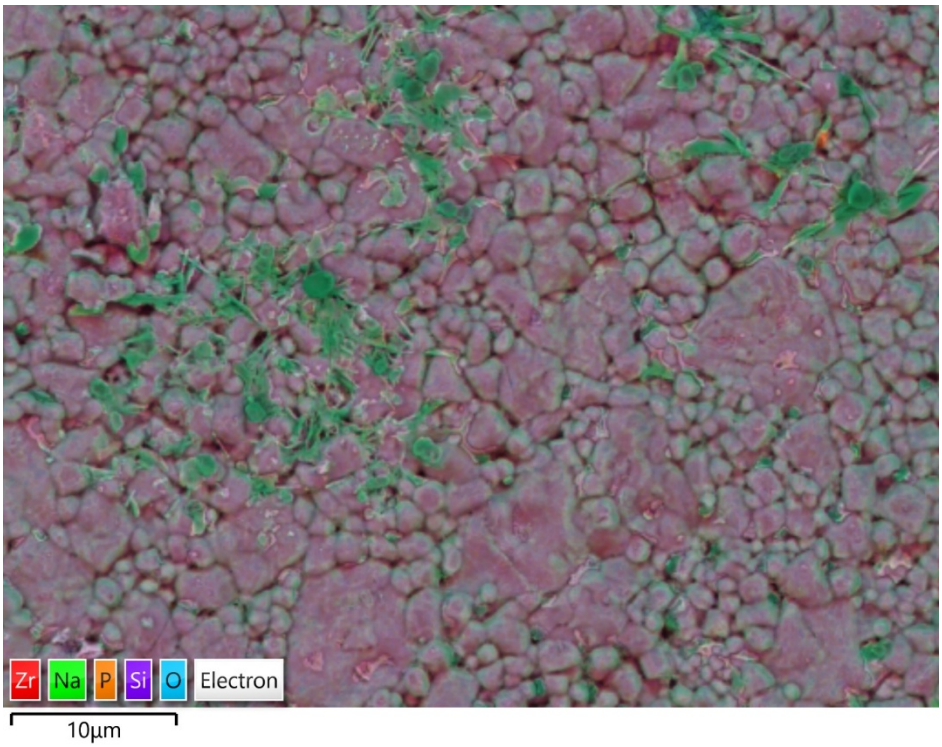

Fig. S4. SEM image and corresponding elemental mapping of the NZSP surface region where the surface dendrite originated (derived from *Adv. Energy Mater.* 202201680). [2]

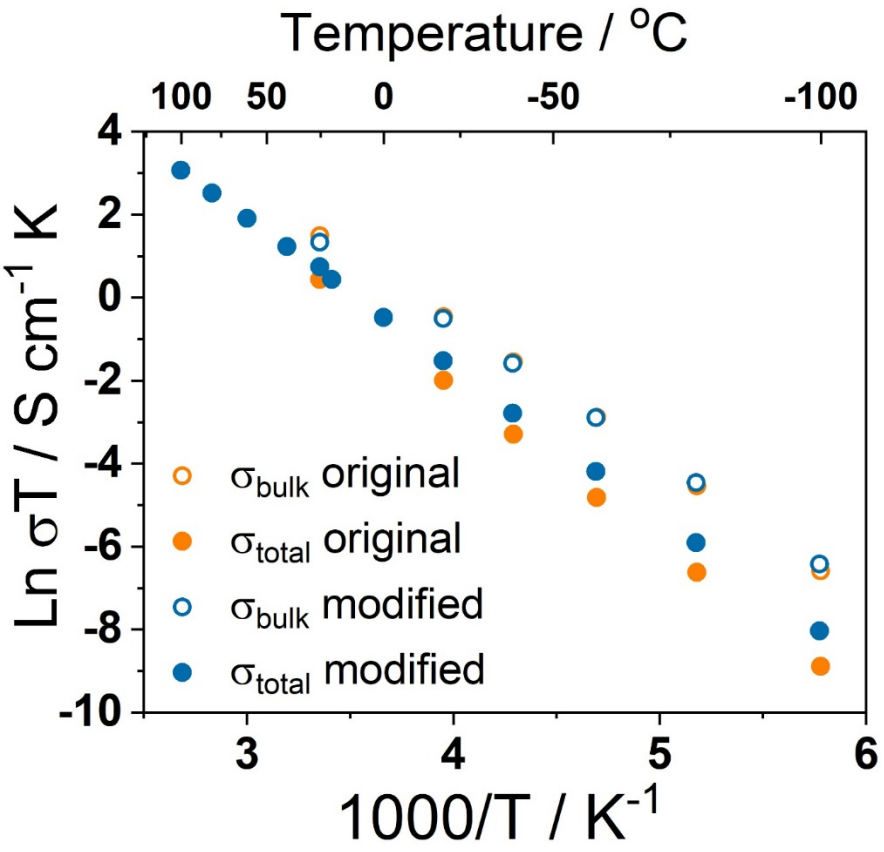

Fig. S5. Arrhenius plot of σ_{total} (filled symbols) and σ_{bulk} (open symbols) of NZSP (orange) and NZSP-2.5NLP (blue). Derived from *J. Power Sources* 626 (2025) 235773. [1]

As shown in Fig. S5, the σ_{bulk} values of original NZSP and NZSP-2.5NLP are very similar in the measured temperature range, indicating that NLP has a negligible influence on the crystal lattice of NZSP. However, the σ_{total} of NZSP-2.5NLP is notably higher than that of NZSP, especially at low temperatures, highlighting the influence of NLP on the grain boundaries of NZSP. This property improvement also affects the activation energy. For σ_{bulk}, the same activation energy of 0.28 eV is determined. In contrast, the activation energy for σ_{total} has a difference of 0.02 eV (0.32 eV for NZSP, 0.30 eV for NZSP-2.5NLP).

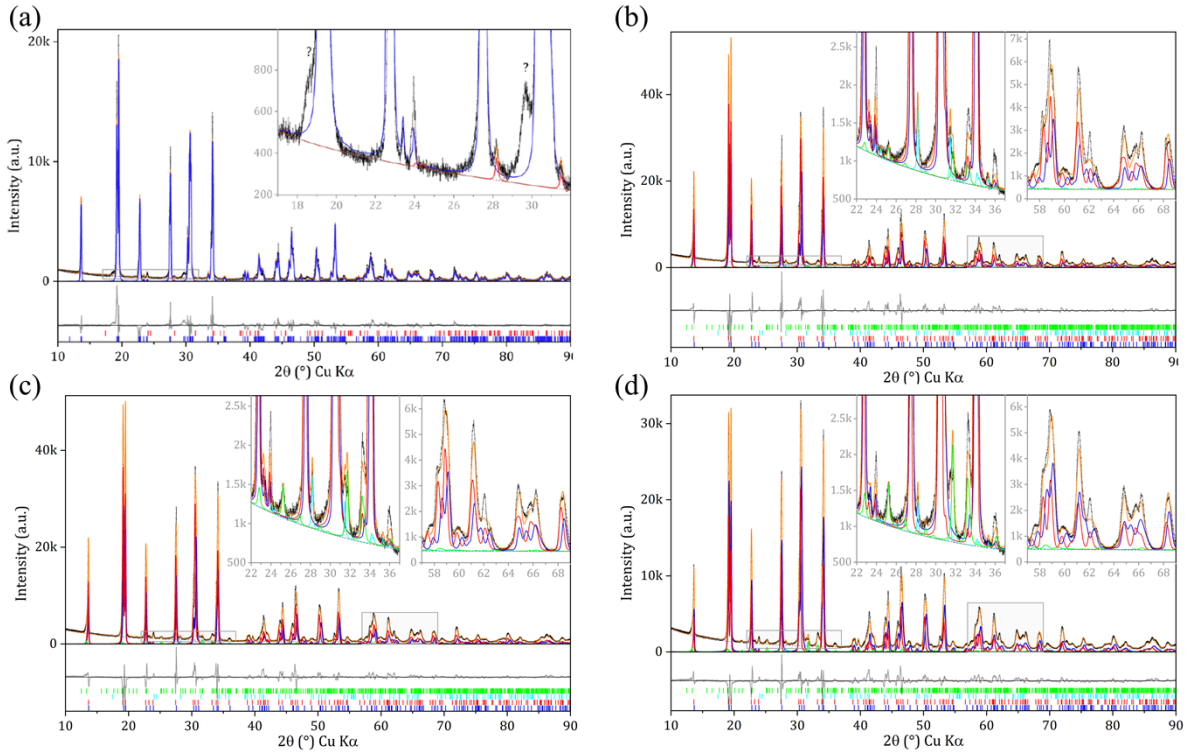

Fig. S6. Rietveld refinement of XRD Data for a) Original NZSP; b) NZSP-1NLP; c) NZSP-2.5NLP and d) NZSP-5NLP. The ICSD numbers are as follows: ZrO_2 (82543 [3]), $Na_3La(PO_4)_2$ (430499 [4]), monoclinic phase of NZSP (38096 [5]) and rhombohedral phase of NZSP (62386 [6]).

In modified NZSP samples, at least two NaSICON-type phases with nearly identical lattice parameters coexist. Due to extensive peak overlap, distinguishing monoclinic and rhombohedral symmetry solely by laboratory XRD data is not reliable. The monoclinic model introduces additional independent lattice parameters (a, b, c and β), which leads to overparameterization without meaningful improvement of refinement indicators. Therefore, the higher-symmetry rhombohedral model, containing only two independent lattice parameters (a,

c), was selected to obtain physically meaningful and stable refinement results.

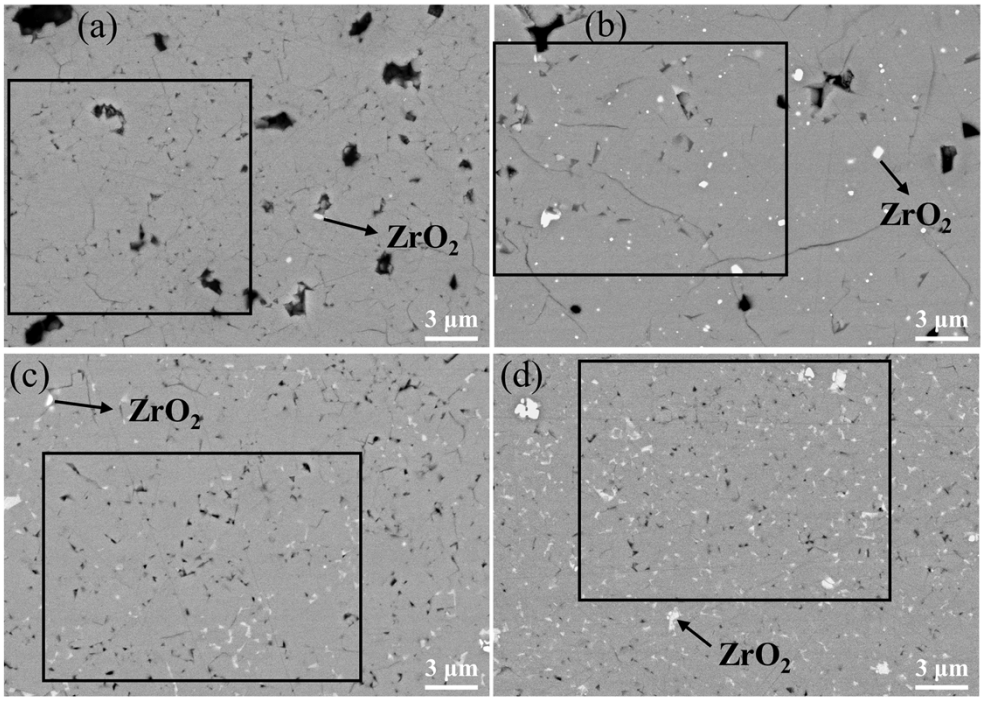

Fig. S7. Backscattered electron SEM images of a) Original NZSP; b) NZSP-1NLP; c) NZSP-2.5NLP and d) NZSP-5NLP. The regions highlighted by black boxes in each subfigure are the image sections extracted and combined to form Fig. 4 in the main text.

Fig. S3 shows the microstructure of the original and modified NZSP. The bright particles correspond to ZrO_2. As seen in Fig. S3(d), the NZSP-5NLP contains a higher amount of ZrO_2, which is consistent with the XRD results.

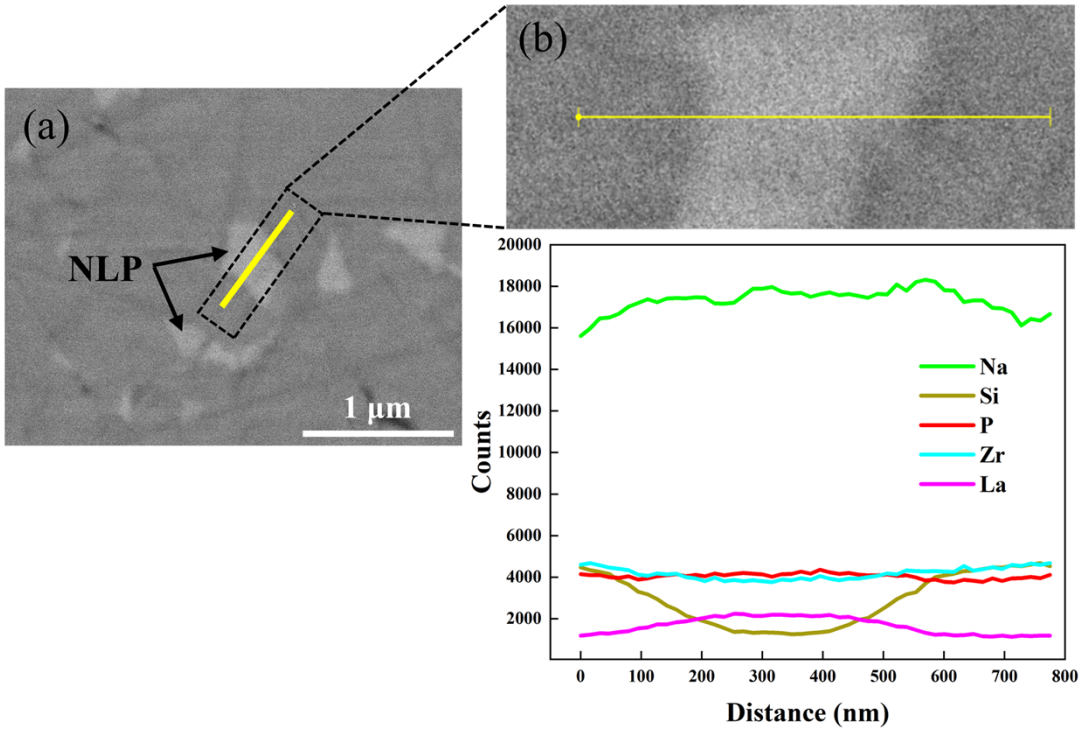

Fig. S8. EDS line-scanning of the interface between NZSP and NLP.

EDS line-scan results in Fig. S4 show a clear peak-shaped enrichment of La at the NZSP/NLP interface, forming a continuous rather than discrete distribution. Na exhibits a similar trend. In contrast, Si displays a distinct interfacial depletion, while P and Zr show slight fluctuations. These elemental variations indicate the presence of a continuous interfacial transition layer between NZSP and NLP, suggesting good interfacial contact.

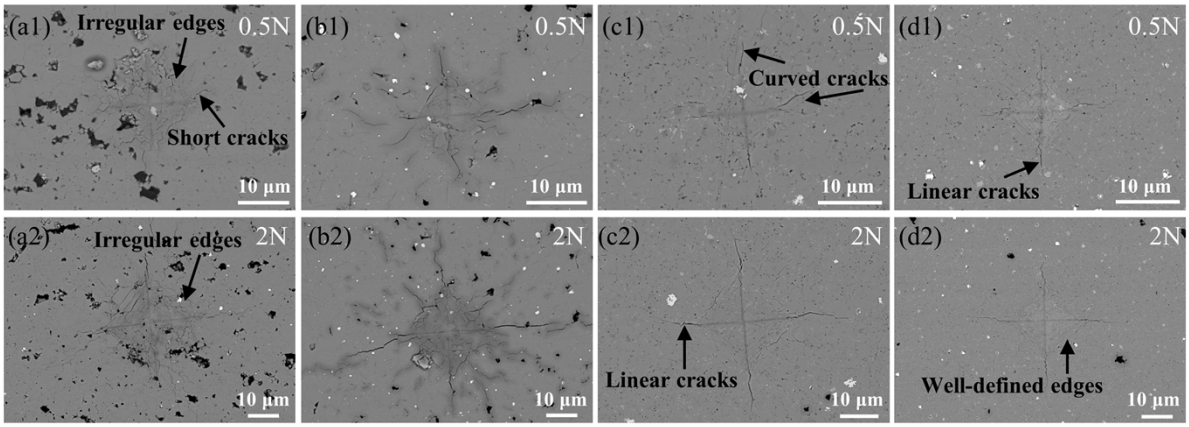

Fig. S9. SEM images of indentation imprints on a1-a2) Original NZSP; b1-b2) NZSP-1NLP; c1-c2) NZSP-2.5NLP and d1-d2) NZSP-5NLP. Note that the imprints are shown at different magnifications as indicated by the scale bars.

At a load of 0.5 N, the original NZSP (Fig. S5a1) exhibited a heavily fractured indentation with irregular edges, and the short, curved cracks could not be measured reliably. By contrast, the NZSP-2.5NLP and NZSP-5NLP samples showed more typical indentation morphologies with well-defined edges and nearly linear cracks. However, the cracks in NZSP-2.5NLP at 0.5 N still displayed noticeable curvature, introducing uncertainty in the accurate determination of their lengths.

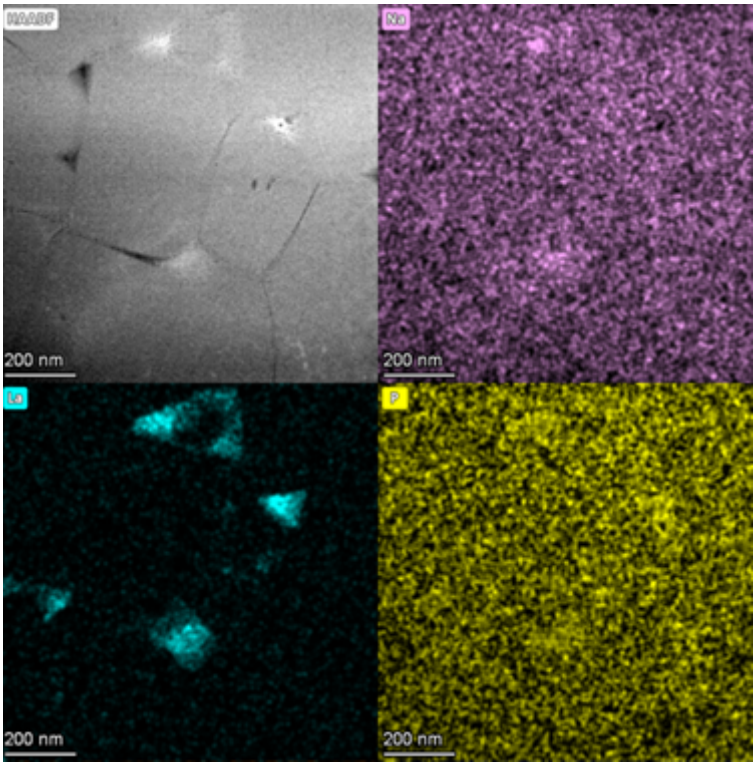

Fig. S10. HAADF-STEM image and corresponding EDX elemental maps of FIB-prepared TEM lamellae of NZSP-2.5NLP. Derived from *J. Power Sources* 626 (2025) 235773. [1]

Through EDX element mapping, areas with enrichment of Na, La and P elements are clearly discernible at which Si and Zr contents are also clearly reduced. The molar ratio of Na: La: P is approximately 3:1:2 within the detection accuracy of EDX element mapping, indicating the existence of NLP in the NZSP ceramic after sintering. All NLP particles are primarily concentrated at the grain boundaries of the ceramic, particularly at the junctions where multiple grains meet.

References

1. L. Liu, Q. Ma, X. Zhou, Z. Ding, D. Grüner, C. Kübel, F. Tietz, *J. Power Sources* **626** (2025) 235773
2. Q. Ma, T. Ortmann, A. Yang, D. Sebold, S. Burkhardt, M. Rohnke, F. Tietz, D. Fattakhova‐Rohlfing, J. Janek, O. Guillon, *Adv. Energy Mater.* **12** (2022) 2201680
3. A. Gualtieri, P. Norby, J. Hanson, J. Hriljac, *J. Appl. Crystallogr.* **29** (1996) 707-713
4. D. Zhao, F. X. Ma, S. Q. Ma, A. Y. Zhang, C. K. Nie, M. Huang, L. Zhang, Y. C. Fan, *Inorg. Chem.* **56** (2017) 1835-1845
5. E. A. Cheung, H. Nguyen, M. Avdeev, N. R. de Souza, Y. S. Meng, N. Sharma, *Chem. Mater.* **33** (2021) 8768-8774
6. J. P. Boilot, G. Collin, P. Colomban, *J. Solid State Chem.* **73** (1988) 160-171